Clinical and Experimental Immunology, 2022, **210**, 309–320
https://doi.org/10.1093/cei/uxac102
Advance access publication 12 November 2022
Research Article

Clinical & Experimental IMMUNOLOGY

OXFORD

Research Article

Exosome-transmitted S100A4 induces immunosuppression and non-small cell lung cancer development by activating STAT3

Xu Wu[1], Hui Zhang[1], Gang Jiang[1], Minlian Peng[1], Cheng Li[1], Jiaxin Lu[1], Shiyin Jiang[1], Xiaoping Yang[2,3,*] and Yongliang Jiang [1,*]

[1]Department of Respiratory Medicine, Hunan Provincial People's Hospital (The First Affiliated Hospital of Hunan Normal University), Changsha, China
[2]Key Laboratory of Study and Discovery of Small Targeted Drugs of Hunan Province, Changsha, China
[3]Department of Pharmacy, School of Medicine, Hunan Normal University, Changsha, China

[*]Correspondence: Yongliang Jiang, Hunan Provincial People's Hospital (The First Affiliated Hospital of Hunan Normal University), No. 61 Jiefang Road, Furong District, Changsha, Hunan Province, China; Email: yvfei316@163.com; Xiaoping Yang, Key Laboratory of Study and Discovery of Small Targeted Drugs of Hunan Province/ School of Medicine, Hunan Normal University, NO. 371 Tongzipo Road, Yuelu District, Changsha, Hunan Province, China; Email: xiaoping.yang@hunnu.edu.cn

Abstract

Non-small cell lung cancer (NSCLC) is the primary reason of tumor morbidity and mortality worldwide. We aimed to study the transfer process of S100A4 between cells and whether it affected NSCLC development by affecting STAT3 expression. First, S100A4 expression in NSCLC cells was measured. The exosomes in MRC-5, A549, and H1299 cells were isolated and identified. We constructed si-S100A4 and si-PD-L1 to transfect A549 cells and oe-S100A4 to transfect H1299 cells, and tested the transfection efficiency. Cell function experiments were performed to assess cell proliferation, clone number, apoptosis, cell cycle, migration, and invasion abilities. In addition, ChIP was applied to determine the targeting relationship between S100A4 and STAT3. Next, we explored NSCLC cell-derived exosomes role in NSCLC progress by transmitting S100A4. Finally, we verified the function of exosome-transmitted S100A4 in NSCLC *in vivo*. High expression of S100A4 was secreted by exosomes. After knocking down S100A4, cell proliferation ability was decreased, clones number was decreased, apoptosis was increased, G1 phase was increased, S phase was repressed, and migration and invasion abilities were also decreased. ChIP validated STAT3 and PD-L1 interaction. After knocking down S100A4, PD-L1 expression was decreased, while ov-STAT3 reversed the effect of S100A4 on PD-L1 expression. Meanwhile, S100A4 inhibited T-cell immune activity by activating STAT3. In addition, knockdown of PD-L1 inhibited cell proliferation, migration, and invasion. NSCLC cell-derived exosomes promoted cancer progression by transmitting S100A4 to activate STAT3 pathway. Finally, *in vivo* experiments further verified that exosome-transmitted S100A4 promoted NSCLC progression. Exosome-transmitted S100A4 induces immunosuppression and the development of NSCLC by activating STAT3.

Received 26 April 2022; Revised 25 August 2022; Accepted for publication 10 November 2022

Graphical Abstract

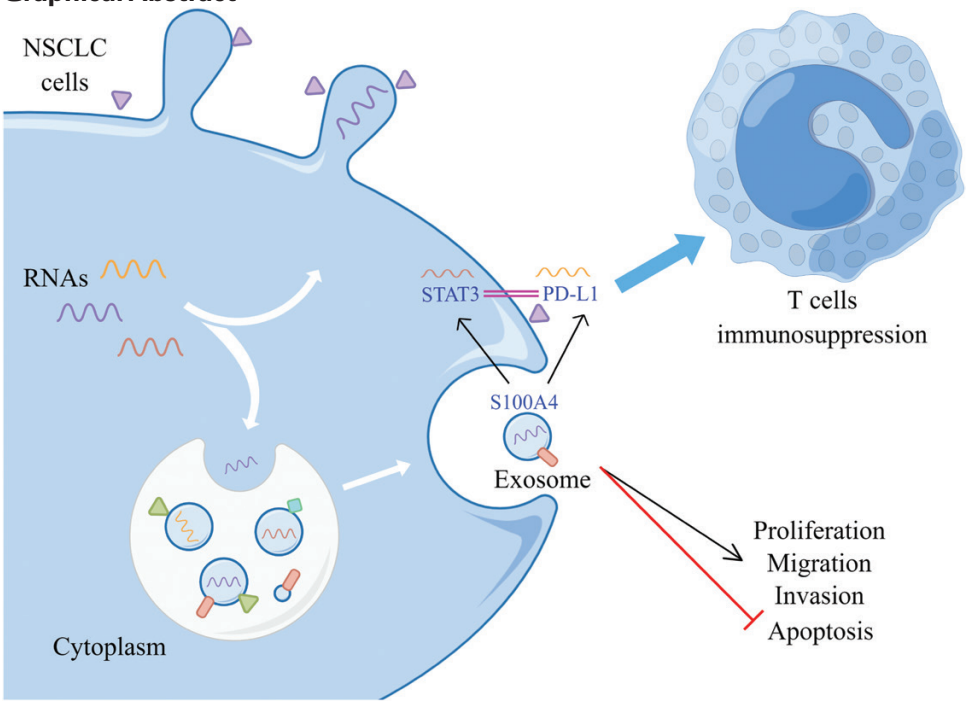

Keywords: exosome, S100A4, STAT3, PD-L1, immunosuppression

Abbreviations: ANOVA: one-way analysis of variance; CCK-8: Cell Counting Kit 8; ChIP: chromatin immunoprecipitation; ex-depleted CM: exosome-depleted conditioned medium; FBS: fetal bovine serum; LC: lung cancer; NSCLC: non-small cell lung cancer; PI: propidium iodide; S100A4: S100 calcium-binding protein A4; SEVs: small extracellular vesicles; TEM: transmission electron microscopy; TLR4: toll-like receptor 4; TRAPs: tumor cell-released autophagosomes.

Introduction

Lung cancer (LC) is a heterogeneous disease. With the deepening of understanding of the molecular changes and genomic biomarkers that drive LC development, traditional LC is divided into small cell LC and non-small cell LC (NSCLC) [1]. NSCLC is a common lethal malignancy, accounting for about 80–85% of lung system tumors [2, 3]. It is the primary reason of tumor morbidity and mortality worldwide [4]. Moreover, the poor prognosis of NSCLC is mainly related to patients being diagnosed at a later stage of the disease [5]. Therefore, there is a pressing demand to find new diagnostic markers and therapeutic approaches.

The S100 protein family is related to various malignant tumors pathogenesis, including lung cancer [6]. S100 calcium-binding protein A4 (S100A4), a member of the S100 family, is widely known for its function in promoting tumor progress and metastasis [7]. S100A4 is an important metastasis-promoting protein driving cancer invasion and metastasis in NSCLC cells [8]. S100A4 plays vital role in NSCLC metastasis and development by regulating adhesion, extracellular matrix remodeling, and cell motility [8–10]. In addition, S100A4 overexpression is related to cancer progress and poor prognosis in NSCLC patients [9]. Therefore, S100A4 may act as the prognostic biomarker for NSCLC. Exosomes are cell-derived nanovesicles ranging in diameter from 30 to 150 nm that are released upon fusion of multivesicular bodies with the cell surface [11]. Exosomes play vital roles in intercellular communication and have oncogenic roles in cancer progress and pre-metastatic niche formation [12]. Exosomes mediate cellular communication in cancer by delivering active molecules and are closely related to tumor proliferation, migration, and immune regulation processes [13]. Oncogenic exosomes contain the factor S100A4, a known regulator of the pre-metastatic niche, enabling us to understand selective differences in exosome composition during tumorigenesis and potential components as prognostic and diagnostic biomarkers in pancreatic cancer [14]. Studies have shown that exosome-mediated S100A4 promotes the development of liver cancer by activating STAT3 [15]. But exosome-mediated S100A4 role in NSCLC is unclear.

In recent years, immunotherapy has proven to be a promising approach to control tumor development. The PD-1/PD-L1 axis produces inhibitory signals that attenuate T cells activity and contribute to tumor immune escape [16, 17]. STAT3 can directly act on PD-L1 promoter to facilitate PD-L1 expression in human tumor cells [13]. As a key target, STAT3 has been widely studied in NSCLC and is mainly related to tumor proliferation, migration, and invasion [18–20]. Furthermore, S100A4 could promote the occurrence of early alcoholic hepatitis by activating the STAT3 pathway [21]. Both S100A4 and STAT3 are related to regulate NSCLC tumor progress, but the link between the two has not been reported.

Based on this, this paper further studies the relationship between S100A4 and STAT3 and the progression of NSCLC, and explores the transmission process of S100A4 between cells and whether it affects NSCLC development by affecting STAT3 expression. Our research may provide novel treatment ideas and targets for NSCLC.

Methods and materials

Cell culture and treatment

Human normal embryonic fibroblasts (MRC-5, CL-0161), NSCLC cell lines A549 (CL-0016), H358 (CL-0400), H1299

(CL-0165), and H460 (CL-0299) were provided by Procell (Wuhan, China). H322 and normal human lung epithelial cells BEAS-2B were provided by ATCC. MRC-5 was cultured in MEM. BEAS-2B was cultured in DMEM. A549 was cultured in Ham's F-12K. H358, H1299, H460, and H322 were cultured in RPMI-1640. These medium all contain 10% fetal bovine serum (FBS), 1% penicillin, and 1% streptomycin. A549 cells were constructed and transfected with si-STAT3 or si-PD-L1 to verify the transfection efficiency. The experimental groupings were: si-NC, si-STAT3; si-NC, si-PD-L1. To further explore the function of STAT3, STAT3 was overexpressed and we grouped cells into NC, si-S100A4, si-S100A4+oe-NC, si-S100A4+oe-STAT3. H1299 cells were incubated with exosomes or exosome-depleted conditioned medium (ex-depleted CM) from A549 cells, and experimental groups were: Control, PBS, A549 Ex, Ex-depleted CM. In addition, we used si-ctrl/si-S100A4 to treat the exosomes extracted from A549 and incubated H1299 cells to detect S100A4 expression. The experimental groupings were: Control, PBS, si-ctrl Ev, si-S100A4 Ev.

Exosome isolation and identification

Exosomes were extracted from MRC-5, A549, and H1299 cell supernatants using an exosome extraction kit (EXOQ5A-1, SBI). The groups were MRC-5 exo, A549 exo, and H1299 exo. Exosomes morphology were analyzed by transmission electron microscopy (TEM). Western blot was applied to determine CD63 (25682-1-AP, 1:1000, proteintech), CD9 (20597-1-AP, 1:1000, proteintech) and Calnexin (66903-1-Ig, 1:5000, proteintech).

Identification and treatment of CD8+ and CD4+ T cells

According to previous literature [22, 23], MagniSort Human CD4 or CD8 T cell Enrichment Kit (8804-6811-74 or 8804-6812-74, ThermoFisher) were applied. Flow cytometry was performed to measure CD4 T and CD8 T cells purity. A549 cells were treated with si-NC/si-S100A4 and then co-cultured with T cells, and CD8+ and CD4+ T cells levels were monitored. The experimental groupings were si-NC and si-S100A4.

Quantitative real-time PCR

Trizol extracted RNA, and RNA was reversed into cDNA by reverse transcription kit (CW2569, Beijing ComWin Biotech, China). cDNA was taken for quantitative PCR. UltraSYBR Mixture Kit (CW2601, Beijing ComWin Biotech, China) was used and PCR was performed on a fluorescence quantitative PCR instrument (QuantStudio1, Thermo). Internal reference of primers was GAPDH, and gene level was calculated by $2^{-\Delta\Delta Ct}$ method. Primer sequences were shown as follows: S100A4-F: TCTTGGTTTGATCCTGACTGC, S100A4-R: TCACCCTCTTTGCCCGAGTA; STAT3-F: CTCTTACTTCTCCAGCAACACT, STAT3-R: ATACATGC TACCTAAGGCCAT; PD-L1-F: TTGCTGAACGCCCC ATACAA, PD-L1-R: TCCAGATGACTTCGGCCTTG; GAPDH-F: ACAGCCTCAAGATCATCAGC, GAPDH-R: GGTCATGAGTCCTTCCACGAT.

Western blot

Protein concentration was determined using RIPA (P0013B, Beyotime), lysis buffer (MB2479, meilunbio), and "BCA" methods. SDS-PAGE loading buffer was mixed and protein was adsorbed on PVDF membrane. S100A4 (16105-1-AP, 1:500, proteintech), cyclin D1 (26939-1-AP, 1:1000, proteintech), BAX (50599-2-Ig, 1:5000, proteintech), Bcl-2 (26593-1-AP, 1:500, proteintech), E-cadherin (20874-1-AP, 1:5000, proteintech), vimentin (10366-1-AP, 1:2000, proteintech), N-cadherin (22018-1-AP, 1:2000, proteintech), twist (11752-1-AP, 1:500, proteintech), slug (12129-1-AP, 1:2000, proteintech), snail (13099-1-AP, 1:500, proteintech), c-Myc (10828-1-AP, 1:5000, proteintech), and β-catenin (51067-2-AP, 1:5000, proteintech), STAT3 (10253-2-AP, 1:1000, proteintech), PD-L1 (17952-1-AP, 1:500, proteintech) and β-actin (66009-1-Ig, 1:1000, proteintech), were incubated overnight at 4°C. Then secondary antibodies were incubated. ECL color exposure. The exposed film was analyzed with quantity One professional grayscale analysis software. β-Actin was used as an internal reference to evaluate protein bands.

Cell Counting Kit 8 assay

Cells were seeded in a 96-well plate at a density of 1×10^4 cells/well and incubated in a 37°C, 5% CO_2 incubator. After culturing adherent treatment for 12, 24, 48, and 72 h, Cell Counting Kit 8 (CCK-8) (10 μl/well, #NU679, DOJINDO, Japan) was added. After incubation at 37°C in 5% CO_2 for 4 h, the absorbance value (450 nm) was analyzed by Bio-Tek microplate reader (MB-530, Heales, China).

Clone formation assay

Cells were digested with 0.25% trypsin digestion solution, and cell suspension was made with serum-free basal medium, and cell density was adjusted to about 1×10^5/ml. One thousand cells/2 ml of each group were cultured in a 37°C, 5% CO_2 incubator for 2–3 weeks. Culture medium was discarded. Four percent paraformaldehyde was fixed, stained with 0.5% crystal violet. Camera took pictures of each well and the clones were counted.

Cell apoptosis and cycle

For apoptosis: cells were collected by centrifugation at 1500 rpm for 5 min. Five hundred and microliters of binding buffer, 5 μl of Annexin V-FITC (# KGA108, keygenbio, Nanjing), and propidium iodide (PI) were added. The reaction was performed at room temperature in the dark for 15 min, and flow cytometry (A00-1-1102, Beckman, USA) was utilized to determine apoptotic cells.

For cell cycle: cell suspension was collected, centrifuged to obtain cell pellet and single-cell suspension, and adjusted to 1×10^6 cells/ml. One hundred and fifty microliters of PI were added and stained in the dark at 4°C for 30 min. Cells were transferred to the flow cytometry detection tube and checked on the flow cytometry. PI was excited by a 488-nm argon-ion laser, received by a 630-nm pass filter, and 10 000 cells were collected by FSC/SSC scattergram. Fragments were analyzed for the percentage of each cell cycle on the PI fluorescence histogram.

Transwell assay

1×10^6/ml cells were resuspended in serum-free medium, and 100 μl of cell suspension and complete medium containing 10% FBS were added to the upper and lower chamber of the transwell chamber (#33318035, Corning), and cultured for 48 h. 4% paraformaldehyde was fixed for 10 min. Cells

were stained with 0.5% crystal violet and eluted with water. Cells on the outer surface of upper chamber were observed under the microscope (Olympus, Japan) and photographed to detect cell migration. For cell invasion, Matrigel Basement Membrane Matrix (BD Biocoat) was used and the rest of the methods were as above. Whether cells entered bottom cavity through small hole was observed with a microscope (Olympus, Japan) and photographed.

Chromatin immunoprecipitation

According to the instructions of the chromatin immunoprecipitation (ChIP) kit, the enrichment of PD-L1 in the STAT3 promoter region was verified. Cells were fixed with 1% formalin for 10 min, then the DNA was randomly fragmented to 200–800 bp by sonication, and the DNA was immunoprecipitated with a target protein-specific antibody against PD-L1. Finally, 100 µl H_2O was used to purify and elute ChIP DNA, and 2.5 µl ChIP-DNA was used for quantitative real-time PCR detection [24]. The enrichment of PD-L1 in the STAT3 promoter was detected.

In vivo tumorigenesis

BALB/c nude mice (male, 21–25 g, 4 weeks, n = 24) were divided into 4 groups: si-ctrl A549, si-S100A4 A549; oe-ctrl H1299, oe-S100A4 H1299, 6 mice in each group. Mice were subcutaneously injected with si-ctrl or si-S100A4-treated A549 cells (2×10^6 cells/cell, 100 µl), and oe-ctrl or oe-S100A4-treated H1299 cells (2×10^6 cells/cell, 100 µl). Tumor volumes were monitored each 4 days; mice were treated after 30 days; tumors were removed and weighed, and tumor weight/volume changes were recorded.

HE staining

Tumor tissue was collected, and HE staining was used to assess histomorphological damage. Slices were baked, dewaxed to water, stained with hematoxylin and eosin, and dehydrated with 95–100% gradient alcohol. After taking them out, slices were placed in xylene for 10 min, 2 times, sealed with neutral gum, and observed under a microscope.

Immunohistochemistry

Immunohistochemistry was utilized to detect S100A4, Ki-67, STAT3, and PD-L1 positive in tissues. Slices were baked, deparaffinized to water, and heated the antigens. S100A4 (16105-1-AP, 1:200, PTG), Ki-67 (ab16667, 1:200, abcam), and PD-L1 (17952-1-AP, 1:200, PTG) primary antibodies were incubated at 4°C overnight, and then secondary antibody was incubated. DAB was applied, and they were counterstained with hematoxylin, and returned to blue with PBS. All levels of alcohol (60–100%) were dehydrated, 5 min per level. After taking them out, they were placed in xylene, and then sealed with neutral gum and observed under a microscope.

TUNEL

In tissue sections, TUNEL Apoptosis Detection Kit (KGA704, KeyGen Biotech, Jiangsu) was applied to evaluate apoptosis in tissues. Briefly, slices were baked and dewaxed to water. One percent of periodic acid blocking solution was prepared, the sections were immersed in the blocking solution, and blocked at room temperature (15–25°C) for 12 min. One hundred and microliters of Proteinase K working solution were added, and reacted at 37°C for 20 min. Biotin (IH0125, Leagene Biotechnology, Beijing) was used for blocking, HRP labeled and observed. DAB (ZLI-9018, ZSGB-BIO, Beijing) was applied, and they were observed under a light microscope.

Statistical analysis

Statistical analysis was performed using Graphpad 8.0. Experimental data were expressed as mean ± SD. Student's t-test or one-way analysis of variance (ANOVA) was used to compare data differences among two or multiple groups. P-value of <0.05 was considered statistically significant.

Results

The high expression of S100A4 was secreted by exosomes

We first measured S100A4 expression in NSCLC cells. Compared with BEAS-2B, S100A4 was highly expressed in NSCLC cell lines. Among them, A549 had the highest expression and H1299 had the lowest expression (Fig. 1A). We then isolated and extracted exosomes from MRC-5, A549, and H1299 cells. Exosome marker detection found that exosomes surface markers CD63, CD9 were all positive, and Calnexin was negative (Fig.1B), which indicated that we successfully extracted exosomes. Finally, we assessed S100A4 expression in exosomes. Compared with MRC-5 exo, S100A4 expression was elevated in A549 exo, and there was no change in

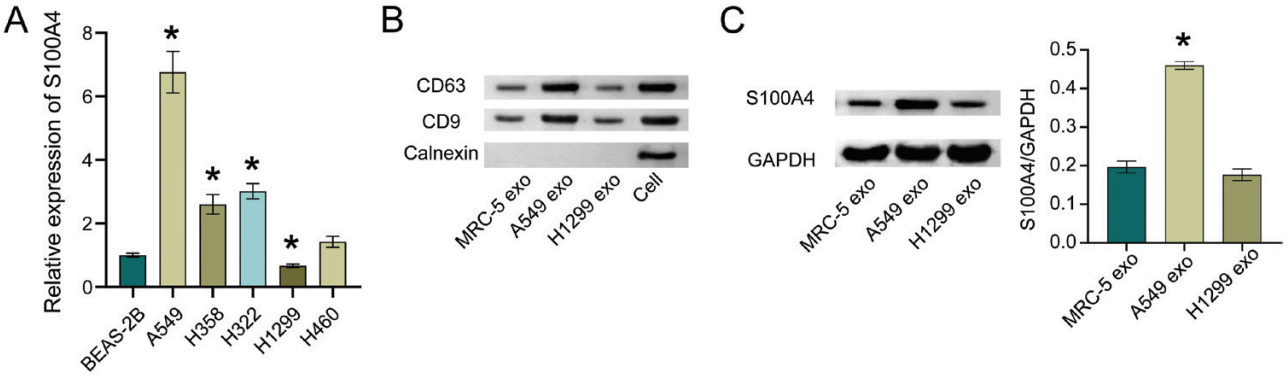

Figure 1: the high expression of S100A4 was secreted by exosomes. A. S100A4 mRNA expression in NSCLC cells. *P < 0.05. B. Exosomes marker CD63, CD9, and Calnexin expressions in exosomes. C. Western blot detection of S100A4 level in exosomes. *P < 0.05.

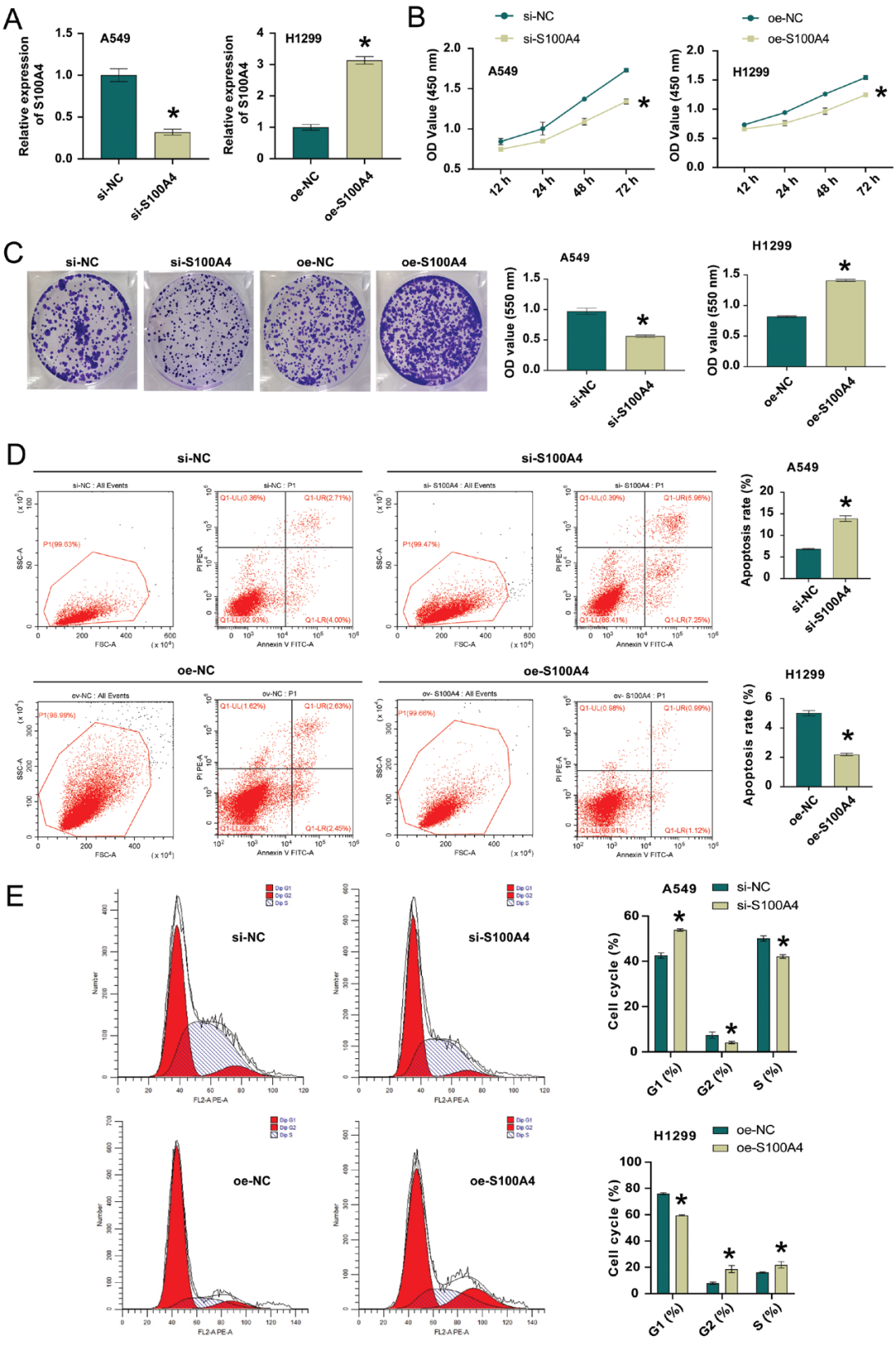

Figure 2: S100A4 regulated the proliferation, migration, and invasion of NSCLC cells. A. S100A4 knockdown or overexpression efficiency in NSCLC cells. B. CCK-8 assay for si-NC, si-S100A4 or oe-NC, oe-S100A4 transfected NSCLC cells. C. Colony formation assay for si-NC, si-S100A4 or oe-NC, oe-S100A4 transfected NSCLC cells. D. The percentage of apoptotic cells in si-NC and si-S100A4 groups. E. Cell cycle distribution in si-NC, si-S100A4 or oe-NC, oe-S100A4 transfected NSCLC cells. F and G. Cyclin D1, Bcl-2, and BAX expression in si-NC, si-S100A4 or oe-NC, oe-S100A4 transfected NSCLC cells. H and I. Transwell migration and invasion assays for si-NC, si-S100A4 or oe-NC, oe-S100A4 transfected NSCLC cells. J and K. E-cadherin, N-cadherin, vimentin, twist, slug, snail, β-catenin, and c-Myc expressions in si-NC, si-S100A4 or oe-NC, oe-S100A4 transfected NSCLC cells. *$P < 0.05$.

S100A4 expression in H1299 exo (Fig. 1C), suggesting that S100A4 was present in the A549 exo.

S100A4 regulated the proliferation, migration, and invasion of NSCLC cells

Next, we constructed si-S100A4 to transfect A549 cells and oe-S100A4 to transfect H1299 cells, and tested the transfection efficiency. Figure 2A showed that the S100A4 knockdown or overexpression was successful. Cell function experiments showed that after knocking down S100A4, cell proliferation ability was decreased, clones number was decreased, apoptosis was increased. Moreover, G1 phase was increased, S phase was repressed, and migration and invasion abilities were also decreased after knocking down S100A4 (Fig. 2B-E and H,I). In addition, after knocking down S100A4, the expression of cell cycle, apoptosis, migration, and invasion-related proteins cyclin D1, Bcl-2, N-cadherin, vimentin, twist, slug, snail, β-catenin, and c-Myc decreased, E-cadherin and BAX expression was increased (Fig. 2F and J). This further validated the results of cell function experiments. The trend of overexpression of S100A4 and interference of S100A4 was opposite. Collectively, S100A4 regulated the proliferation, migration, and invasion processes of NSCLC cells.

S100A4 regulated PD-L1 expression and inhibited T-cell immune activity by activating STAT3

Next, we assessed STAT3 and PD-L1 levels. Compared with si-NC group, PD-L1 and STAT3 levels were reduced in the si-S100A4 group (Fig. 3A). In addition, A549 cells were treated with si-NC/si-S100A4 and then co-cultured with T cells, and CD8+ and CD4+ T cells levels were detected. Compared with si-NC group, the si-S100A4 group had elevated levels of CD8+ T and CD4+ T cells (Fig. 3B). Then we constructed si-STAT3 in A549 cells. Figure 3C showed successful interference with STAT3. ChIP validated the interaction between STAT3 and PD-L1 (Fig. 3D). Next, we overexpressed STAT3 while interfering with S100A4. Figure 3E suggested PD-L1 expression was decreased after interfering with S100A4, while oe-STAT3 reversed the effect of S100A4 on PD-L1 expression. Finally, we knocked down PD-L1. Figure 3F showed successful interference with PD-L1. Cell function experiments showed that after PD-L1 was knocked down, the cell proliferation ability decreased, and the migration and invasion abilities were also reduced (Fig. 3G–I). In general, S100A4 regulated PD-L1 expression and inhibited T-cell immune activity by targeting STAT3.

Exosome-transmitted S100A4 promoted NSCLC progression by targeting STAT3

To explore NSCLC cell-derived exosomes role in cancer progression by delivering S100A4, we incubated H1299 cells with exosomes from A549 cells or exosome-depleted conditioned medium (ex-depletion CM), or we used si-ctrl/si-S100A4 to treat the exosomes extracted from A549 and incubate with H1299 cells to detect S100A4 expression. As shown in Fig. 4A–C, S100A4 expression was elevated in both A549 Ex or si-ctrl Ev groups than PBS group. Ex-depleted CM or si-S100A4 Ev group reversed the effect of A549 Ex

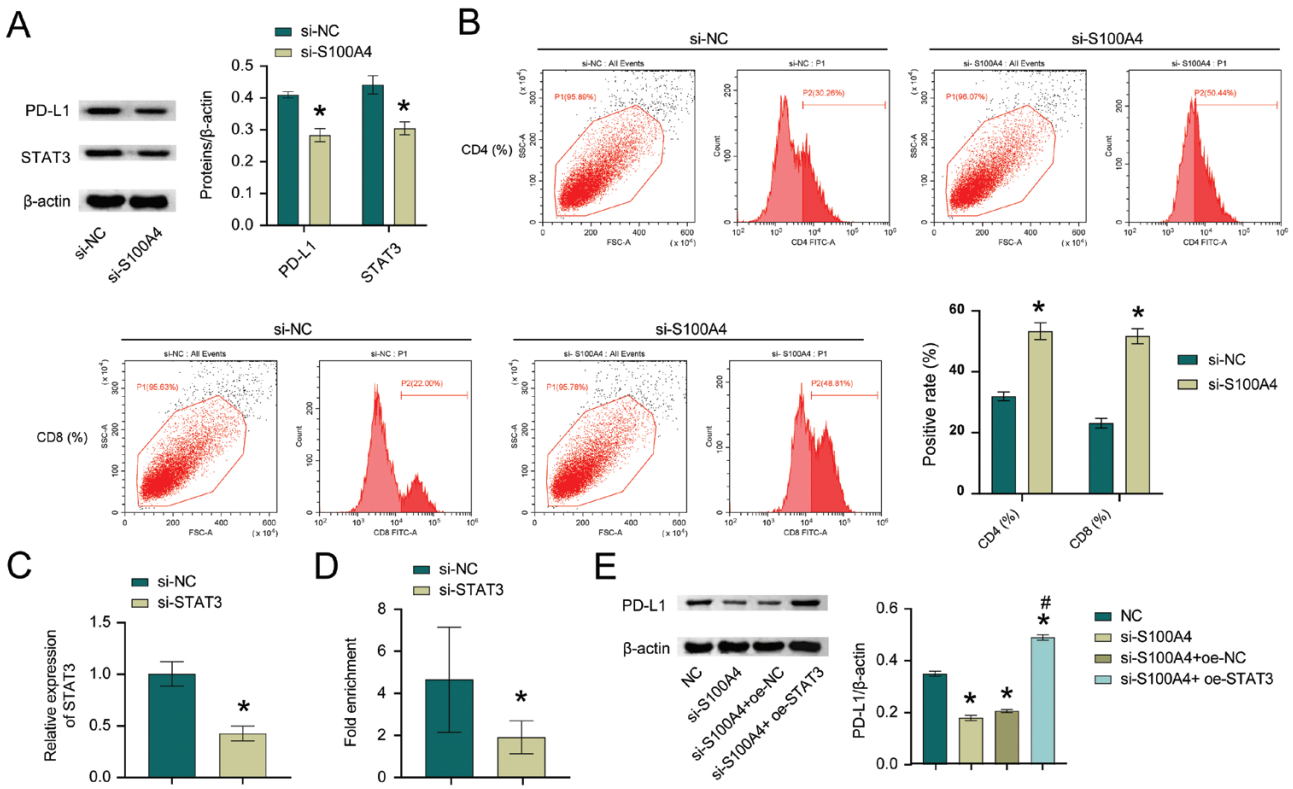

Figure 3: S100A4 regulated PD-L1 expression and inhibited T-cell immune activity by activating STAT3. A. Western blot measured STAT3 and PD-L1 levels. *$P < 0.05$. B. The effect of different treatments on CD4+ and CD8+ populations among A549 cells. C. STAT3 knockdown efficiency in A549 cells. *$P < 0.05$. D. ChIP was utilized to verify STAT3 binding to PD-L1. E. PD-L1 protein level. *$P < 0.05$ vs NC, #$P < 0.05$ vs si-S100A4+oe-STAT3. *$P < 0.05$. F. PD-L1 knockdown efficiency in A549 cells. *$P < 0.05$. G. CCK-8 assay for si-NC and si-PD-L1 transfected NSCLC cells. H and I. Transwell migration and invasion assays for si-NC and si-PD-L1 transfected NSCLC cells. *$P < 0.05$.

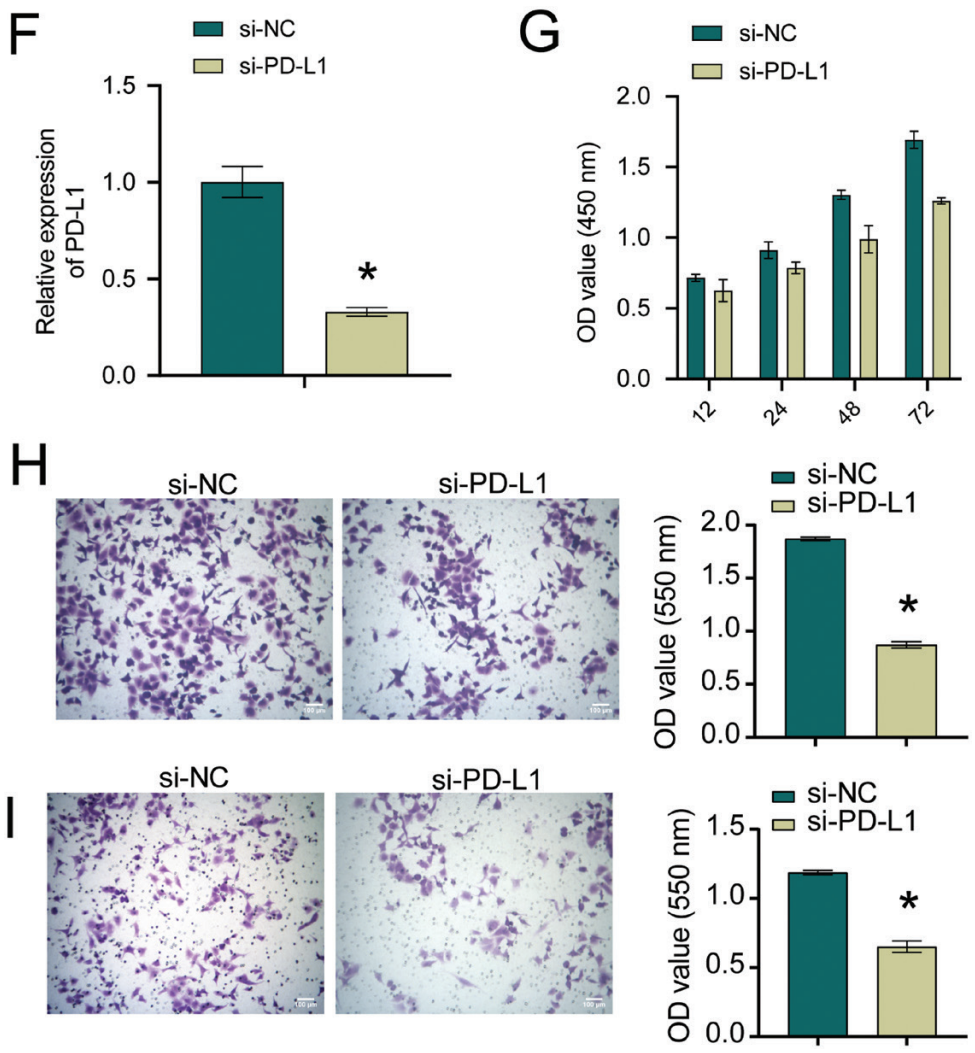

Figure 3: Continued

or si-ctrl Ev on S100A4 expression. Next, we assessed STAT3 and PD-L1 levels. Compared with the PBS group, PD-L1 and STAT3 expressions were elevated in the A549 Ex or si-ctrl Ev groups. These expressions were reversed after the use of Ex-depleted CM or si-S100A4 Ev (Fig. 4D–F). Cell function experiments suggested H1299 cells in the A549 Ex or si-ctrl Ev group had increased cell proliferation, increased clone number, and increased migration and invasion levels than PBS group (Fig. 4G–J). In contrast, these functions were reduced with Ex-depleted CM or si-S100A4 Ev. These results indicated exosome-transmitted S100A4 promoted NSCLC progression by targeting STAT3.

Exosome-derived S100A4 promotes NSCLC progression *in vivo*

Finally, we validated the function of exosome-derived S100A4 in NSCLC *in vivo*. Fig. 5A–C showed tumor size, weight, and volume. Compared with si-ctrl A549, si-S100A4 A549 group had decreased tumor weight and volume. Tumor weight and volume in the oe-S100A4 H1299 group increased than oe-ctrl H1299 group. HE staining results showed that inflammatory cell infiltration was decreased after si-S100A4, whereas inflammatory cell infiltration was increased after oe-S100A4 (Fig. 5D). After si-S100A4, Ki-67 expression was suppressed and apoptosis was facilitated. However, after oe-S100A4, Ki-67 expression was promoted and apoptosis was repressed (Fig. 5E, F). In addition, S100A4 and PD-L1 expressions were also repressed after si-S100A4, whereas S100A4 and PD-L1 expressions were promoted after oe-S100A4 (Fig. 5G). These results revealed exosome-derived S100A4 promoted NSCLC progression.

Discussion

NSCLC is an aggressive disease and one of the diseases with poor prognosis in cancer [25]. Molecular testing has now become a mandatory component of NSCLC management [26]. In recent years, targeting the immune system to achieve meaningful clinical benefits has been demonstrated successfully in various malignancies [27]. Therefore, the application of immunotherapy in NSCLC has received renewed attention. In this paper, cancer cells in NSCLC communicated with each other through exosome-transmitted S100A4, induced STAT3 expression, activated PD-1/PD-L1 signaling, and inhibited T cells activity to produce immunosuppression, promote the development of NSCLC and produce poor disease prognosis.

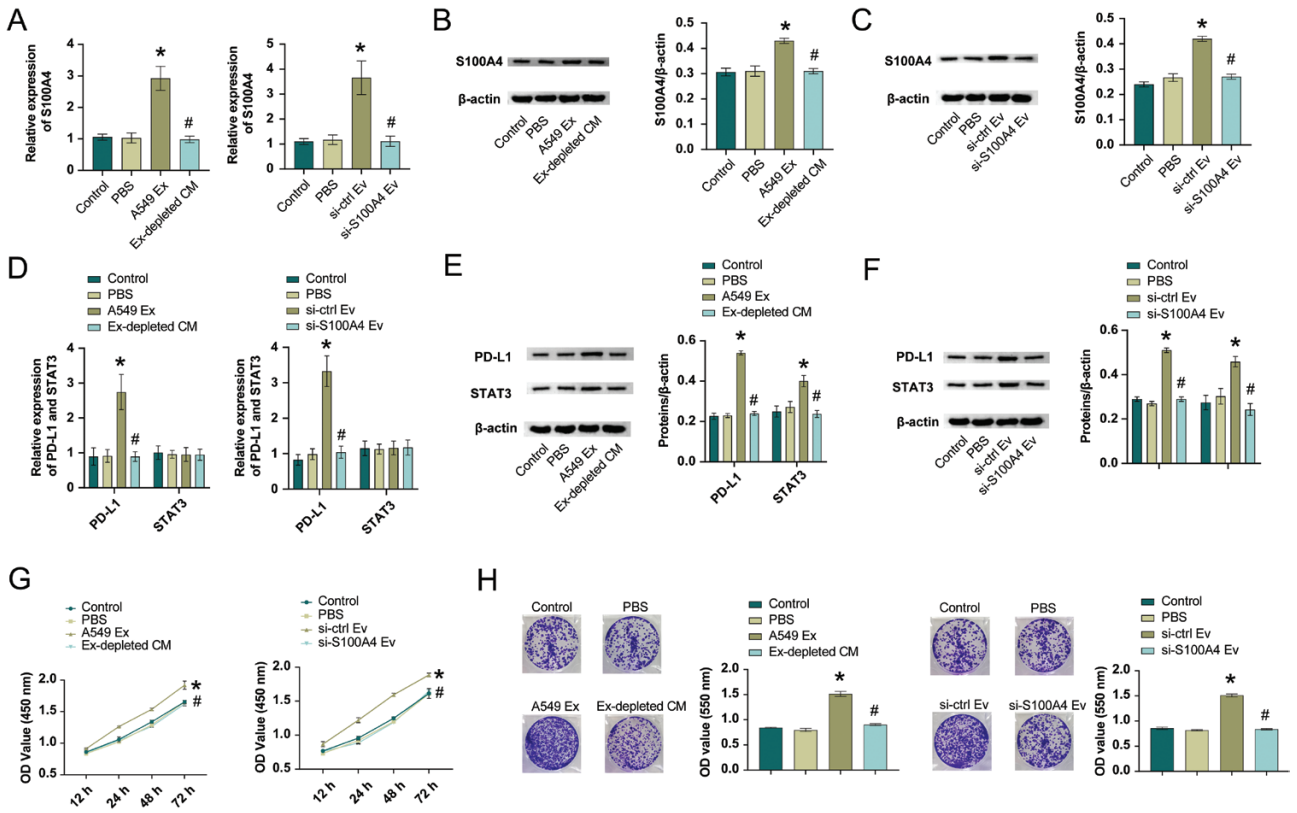

Figure 4: exosome-transmitted S100A4 promoted NSCLC progression by targeting STAT3. A–C. S100A4 mRNA and protein level. D–F. STAT3 and PD-L1 mRNA and protein levels. CCK-8 (G), colony formation (H), transwell migration (I), and invasion (J) assays for A549 cells treated with PBS, Ex-depleted CM, or exosomes from sh-Ctrl and sh-S100A4 transfected A549 cells. *$P < 0.05$ vs PBS, # $P < 0.05$ vs A549 Ex or si-ctrl Ev.

S100A4 expression was observed in 81 of 135 NSCLC cases (60%) and was associated with pathological T-factor progression, lymph node metastasis, and poor survival [28]. Qi et al. reported that in 116 patients, S100A4 protein immunohistochemistry was positive in 64 cases, and the positive rate was 55.2%. S100A4 protein expression was related to the age, tumor size, lymph node metastasis, and NSCLC prognosis [29]. In most S100A4 publications, S100A4 has a slight effect on tumor cell proliferation. It has been reported that knockdown of S100A4 resulted in reduced proliferation and migration of gastric cancer cells [30]. Overexpression of S100A4 promoted the proliferation of endometrial cancer cells and inhibited apoptosis [31]. Knockdown of S100A4 inhibited bladder cancer cell proliferation, migration, invasion and tumor growth [32]. Consistent with our study, high expression of S100A4 was secreted through exosomes. In addition, we found that after interfering with S100A4, the cell proliferation ability was decreased, the number of clones was decreased, the apoptosis was increased, the G1 phase was elevated, S phase was repressed, and the level of migration and invasion was also decreased. This suggests that S100A4 may be used as a biomarker for diagnosing and treating NSCLC.

Studies have shown that exosomes from bone marrow mesenchymal stem cells facilitate the proliferation, invasion, and chemoresistance of leukemia cells by upregulating S100A4 [33]. Our study found that exosomes extracted from NSCLC cells with high expression of S100A4 could promote the proliferation, migration, and invasion of NSCLC cells. This is the first time we report the role of exosome-transmitted S100A4 in NSCLC, which is also the innovation of our article. Meanwhile, through *in vivo* experiments, we further verified that exosome-derived S100A4 promoted NSCLC progression. In this work, we first explored the non-exosome-mediated effects of S100A4 on cell proliferation, migration, invasion, and apoptosis. As shown in Fig. 2, knockdown of S100A4 inhibited cell proliferation, migration and invasion, and promoted cell apoptosis. Overexpression of S100A4 promoted cell proliferation, migration and invasion, and reduced apoptosis. The results indicated that S100A4 induced cell proliferation, migration and invasion, and reduced apoptosis. It has been reported that exosomes are a subset of the tumor microenvironment that deliver nucleic acids, proteins, and lipids to facilitate intercellular communication and activate signaling pathways in target cells [34]. Our results showed that A549 Ex increased S100A4 expression in H1299 cells, while Ex-depletion CM or si-S100A4 Ev abrogated the effect of A549 Ex or si-ctrl Ev on S100A4 expression. The results indicated that the amount of non-exosome sources of S100A4 was small. S100A4 might be mainly delivered to H1299 cells through exosomes. Our findings further showed that A549 cell-derived exosomes promoted cell proliferation, migration and invasion, while exosomes depletion and knockdown of S100A4 A549 cell-derived exosomes abolished the effect of S100A4 on cell function. The results indicated that tumor cells mainly affected cell proliferation, migration, and invasion through exosomes-secreted S100A4. Exosomes are derived from almost all types of cells and are present in all body fluids. Due to their amphiphilic structure, exosomes are natural drug delivery vehicles for cancer therapy [35–37]. Exosomes have

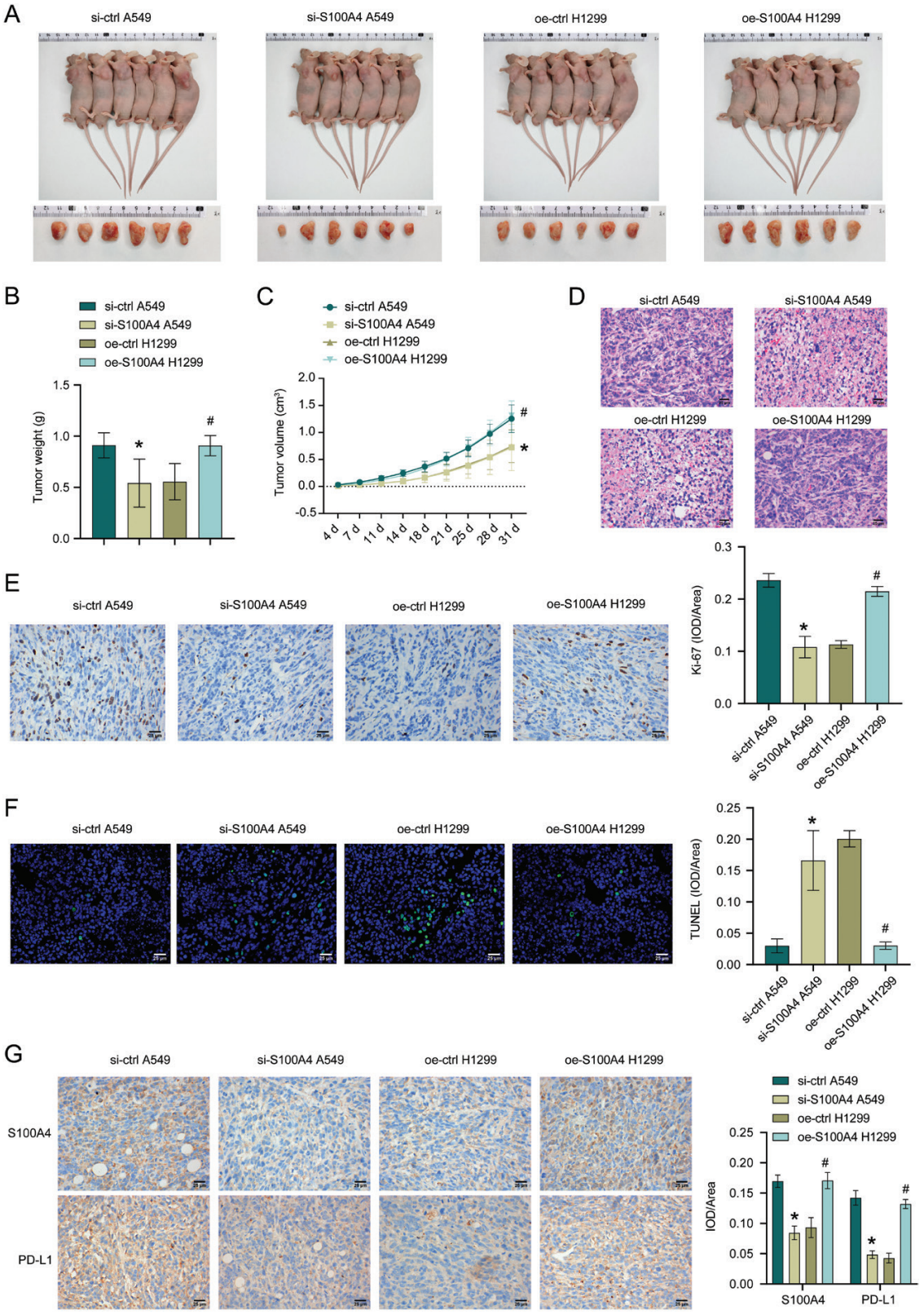

Figure 5: exosome derived S100A4 promotes NSCLC progression *in vivo*. A–C. Tumor size, weight, and volume of mice injected with A549 cells treated with si-ctrl or si-S100A4 and H1299 cells transfected with oe-ctrl or oe-S100A4. D–F. HE, Ki-67, and TUNEL staining in tumor tissues. G. Immunohistochemistry assay for detecting S100A4 and PD-L1 expressions. *$P < 0.05$ vs PBS, #$P < 0.05$ vs A549 Ex or si-ctrl Ev.

good homologous targeting ability and significantly improve delivery efficiency; engineered exosomes loaded with miR-449a selectively inhibit the growth of NSCLC [38]. Our results are consistent with previous studies. S100A4-loaded exosomes might serve as a promising therapeutic strategy for NSCLC.

Various cytokines found in the immunoreactive microenvironment-induced PD-L1 level on cancer and/or immune cells via different signaling mechanisms [39]. In NSCLC, microRNA-4458 overexpression enhances antitumor immunity by targeting STAT3 to intercept PD-L1/PD-1 pathway [40]. Studies have confirmed that the AKT–STAT3 pathway might be the potential targets for regulating PD-L1 level on the surface of NSCLC with abnormal EGFR activity, and inhibiting AKT or STAT3 activity repressed PD-L1 level in gefitinib-resistant NSCLC [41]. We validated the interaction between STAT3 and PD-L1 by ChIP. STAT3 plays vital roles in cancer progress as a driver oncogene and as a selectively activated pathway to acquire resistance to targeted therapy [42]. The roles of S100A4 and STAT3 in NSCLC have been reported in the literature, which also provides a basis for the feasibility of this paper. We illuminated S100A4 regulated PD-L1 expression and inhibited T-cell immune activity by activating STAT3. Meanwhile, NSCLC cell-derived exosomes promoted cancer progression by delivering S100A4 to target the STAT3 pathway. This suggests that the promotion of tumor development by S100A4 may be related to the activation of STAT3/PD-L1 signaling leading to immunosuppression.

The previous study has shown that S100A4 protected myeloid-derived suppressor cells from intrinsic apoptosis through Toll-like receptor 4 (TLR4)-ERK1/2 signaling [43]. The abundance of S100A4 in exosomes derived from olfactory extracellular mesenchymal stem cells mediated the endogenous production of IL-6 by myeloid-derived suppressor cells through TLR4 signaling, thereby ameliorating murine Sjögren's syndrome [44]. TLR4 plays a pivotal role in the tumor immune microenvironment [45]. It has been reported that activation of TLR4 might induce the expression of PD-L1 through the ERK signaling pathway, thereby promoting NSCLC progression [46]. Morphine-3-glucuronide upregulated PD-L1 expression and promotes immune escape in NSCLC via TLR4 [47]. We speculate that S100A4 induces immunosuppression and promotes NSCLC progression through PD-L1/STAT3, possibly related to TLR4-ERK1/2 signaling. In the next project, we will further explore the underlying molecular mechanism by which S100A4 induces immunosuppression and promotes NSCLC progression through PD-L1. The previous study has shown that tumor cell-released autophagosomes (TRAPs) inhibited the proliferation of CD4+ and CD8+ T cells through TLR4-mediated MyD88-p38-STAT3 signaling, increased PD-L1 expression, and then promoted cancer progression [48]. Tumor-derived small extracellular vesicles (SEVs) upregulated PD-L1 and activated STAT3 signaling through the TLR4/NF-κB pathway, thereby inducing immunosuppression and tumorigenesis [49]. We speculate that S100A4 might affect immune escape and NSCLC progression by activating the STAT3 signaling pathway through the TLR4/NF-κB pathway. In the next project, we will further investigate the underlying molecular mechanism by which S100A4 induces immunosuppression and promotes NSCLC progression through PD-L1/STAT3. S100A4 is a major inducer of cancer progression and metastasis [50]. Knockdown of S100A4 inhibited prostate cancer tumor growth by inhibiting angiogenesis [51]. S100A4 promoted bladder cancer stem cell proliferation and accelerated tumor growth by activating the IKK/NF-κB signaling pathway, while knockdown of S100A4 showed the opposite effect [52]. Estrogen-related receptor γ promoted migration, invasion and tumor growth of endometrial cancer cells by targeting S100A4 [53]. In this project, *in vivo* results showed that knockdown of S100A4 reduced tumor mass and slowed tumor volume increase. Overexpression of S100A4 increased tumor mass and promoted tumor volume. Our results preliminarily clarified the promoting effect of S100A4 on NSCLC tumor growth. In the next project, we will further explore whether S100A4 affects tumor metastasis in NSCLC through exosomal delivery by intravenous injection of tumor cells and the underlying molecular mechanism. We have supplemented images of animal and tumor. A larger sample size may yield better convincing results. Refer to previous research [54–57], we had six animals per group considering the limited funding. The results showed that the differences between the groups were relatively obvious, which clarified the role of S100A4 in NSCLC tumors growth. In the next project, we will increase the number of animals to further explore the potential molecular mechanism of S100A4 in NSCLC.

Conclusion

In conclusion, the innovation of this paper is to further study the relationship between S100A4 and STAT3 and the progression of NSCLC. We found that exosome-transmitted S100A4 induced immunosuppression and NSCLC development by targeting STAT3. This research provides novel idea for studying NSCLC and therapeutic target for treating NSCLC.

Acknowledgements

The authors would like to acknowledge the FiGDRAW software. The graphical abstract is drawn using FiGDRAW software. ID for ITOTP85885.

Funding

This work was supported by the National Natural Science Foundation of China, China (82070057), project funded by China Postdoctoral Science Foundation(2022M711124), Natural Science Foundation of Hunan Province, China (2022JJ40227, 2021JJ30400), and Natural Science Foundation of Changsha (kq2014191).

Conflict of interests

The authors declare that they have no conflicts of interest.

Author contributions

Xu Wu, Hui Zhang, Minlian Peng, Cheng Li, and Xiaoping Yang participated in the conception and design of the study. Hui Zhang, Jiaxin Lu, Shiyin Jiang and Yongliang Jiang acquired data, performed the statistical analysis. Xu Wu and Xiaoping Yang interpreted the results and wrote the initial version of the manuscript. Gang Jiang contributions to data aggregation, validation and analysis of experimental results. All authors critically revised the manuscript and approved the final version.

Ethical approval

This study was approved by the Animal Ethics Committee of Hunan Provincial People's Hospital. The animal research

adheres to the ARRIVE guidelines. The treatment of animals during the experiment conforms to the standards of "Guiding Opinions on Being kind to Experimental Animals" issued by the Ministry of Science and Technology in 2006.

Data availability

The datasets used and/or analyzed during the current study are available from the corresponding author on reasonable request.

References

1. Tan AC. Targeting the PI3K/Akt/mTOR pathway in non-small cell lung cancer (NSCLC). *Thorac Cancer* 2020, 11, 511–8. doi:10.1111/1759-7714.13328.
2. Suster DI, Mino-Kenudson M. Molecular pathology of primary non-small cell lung cancer. *Arch Med Res* 2020, 51, 784–98. doi:10.1016/j.arcmed.2020.08.004.
3. Azghadi S, Daly ME. Radiation and immunotherapy combinations in non-small cell lung cancer. *Cancer Treat Res Commun* 2021, 26, 100298. doi:10.1016/j.ctarc.2020.100298.
4. Marmarelis ME, Langer CJ. Treatment of patients with non-small-cell lung cancer harboring rare Oncogenic mutations. *Clin Lung Cancer* 2020, 21, 395–406. doi:10.1016/j.cllc.2020.01.010.
5. Baran K, Brzeziańska-Lasota E. Proteomic biomarkers of non-small cell lung cancer patients. *Adv Respir Med* 2021, 89, 419–26. doi:10.5603/ARM.a2021.0089.
6. Wang T, Du G, Wang D. The S100 protein family in lung cancer. *Clin Chim Acta* 2021, 520, 67–70. doi:10.1016/j.cca.2021.05.028.
7. Fei F, Qu J, Li C, Wang X, Li Y, Zhang S. Role of metastasis-induced protein S100A4 in human non-tumor pathophysiologies. *Cell Biosci* 2017, 7, 64. doi:10.1186/s13578-017-0191-1.
8. Liu L, Qi L, Knifley T, Piecoro DW, Rychahou P, Liu J, et al. S100A4 alters metabolism and promotes invasion of lung cancer cells by up-regulating mitochondrial complex I protein NDUFS2. *J Biol Chem* 2019, 294, 7516–27. doi:10.1074/jbc.RA118.004365.
9. Zhang J, Gu Y, Liu X, Rao X, Huang G, Ouyang Y. Clinicopathological and prognostic value of S100A4 expression in non-small cell lung cancer: a meta-analysis. *Biosci Rep* 2020, 40, BSR20201710. doi:10.1042/BSR20201710.
10. Stewart RL, Carpenter B, West DS, Knifley T, Liu L, Wang C, et al. S100A4 drives non-small cell lung cancer invasion, associates with poor prognosis, and is effectively targeted by the FDA-approved anti-helminthic agent niclosamide. *Oncotarget* 2016, 7, 34630–42.
11. Wu H, Mu X, Liu L, Wu H, Hu X, Chen L, et al. Bone marrow mesenchymal stem cells-derived exosomal microRNA-193a reduces cisplatin resistance of non-small cell lung cancer cells via targeting LRRC1. *Cell Death Dis* 2020, 11, 801. doi:10.1038/s41419-020-02962-4.
12. Kalluri R. The biology and function of exosomes in cancer. *J Clin Invest* 2016, 126, 1208–15. doi:10.1172/JCI81135.
13. Zhang L, Yu D. Exosomes in cancer development, metastasis, and immunity. *Biochim Biophys Acta Rev Cancer* 2019, 1871, 455–68. doi:10.1016/j.bbcan.2019.04.004.
14. Emmanouilidi A, Paladin D, Greening DW, Falasca M. Oncogenic and non-malignant pancreatic exosome cargo reveal distinct expression of oncogenic and prognostic factors involved in tumor invasion and metastasis. *Proteomics* 2019, 19, e1800158. doi:10.1002/pmic.201800158.
15. Sun H, Wang C, Hu B, et al. Exosomal S100A4 derived from highly metastatic hepatocellular carcinoma cells promotes metastasis by activating STAT3. *Signal Transduct Target Ther* 2021, 6, 187.
16. Li H, Li C, Li X, Ding Q, Guo L, Liu S, et al. MET inhibitors promote liver tumor evasion of the immune response by stabilizing PDL1. *Gastroenterology* 2019, 156, 1849–1861.e13. doi:10.1053/j.gastro.2019.01.252.
17. Jiao S, Xia W, Yamaguchi H, Wei Y, Chen MK, Hsu JM, et al. PARP inhibitor upregulates PD-L1 expression and enhances cancer-associated immunosuppression. *Clin Cancer Res* 2017, 23, 3711–20. doi:10.1158/1078-0432.CCR-16-3215.
18. Chen B, Ling C. Long noncoding RNA AK027294 acts as an oncogene in non-small cell lung cancer by up-regulating STAT3. *Eur Rev Med Pharmacol Sci* 2019, 23, 1102–7. doi:10.26355/eurrev_201902_17000.
19. Ren W, Hou J, Yang C, Wang H, Wu S, Wu Y, et al. Extracellular vesicles secreted by hypoxia pre-challenged mesenchymal stem cells promote non-small cell lung cancer cell growth and mobility as well as macrophage M2 polarization via miR-21-5p delivery. *J Exp Clin Cancer Res* 2019, 38, 62. doi:10.1186/s13046-019-1027-0.
20. Zhu H, Chang L, Yan FJ, Hu Y, Zeng CM, Zhou TY, et al. AKR1C1 activates STAT3 to promote the metastasis of non-small cell lung cancer. *Theranostics* 2018, 8, 676–92. doi:10.7150/thno.21463.
21. Yuan Q, Hou S, Zhai J, Tian T, Wu Y, Wu Z, et al. S100A4 promotes inflammation but suppresses lipid accumulation via the STAT3 pathway in chronic ethanol-induced fatty liver. *J Mol Med (Berl)* 2019, 97, 1399–412. doi:10.1007/s00109-019-01808-7.
22. Yang J, Yan J, Shao J, Xu Q, Meng F, Chen F, et al. Immune-mediated antitumor effect By VEGFR2 selective inhibitor for gastric cancer. *Onco Targets Ther* 2019, 12, 9757–65. doi:10.2147/OTT.S233496.
23. Zhu Q, Yuan J, He Y, Hu Y. The effect of miR-520b on macrophage polarization and T cell immunity by targeting PTEN in breast cancer. *J Oncol* 2021, 2021, 5170496. doi:10.1155/2021/5170496.
24. Wang Q, Xu L, Zhang X, Liu D, Wang R. GSK343, an inhibitor of EZH2, mitigates fibrosis and inflammation mediated by HIF-1α in human peritoneal mesothelial cells treated with high glucose. *Eur J Pharmacol* 2020, 880, 173076. doi:10.1016/j.ejphar.2020.173076.
25. Di Paolo A, Del Re M, Petrini I, Altavilla G, Danesi R. Recent advances in epigenomics in NSCLC: real-time detection and therapeutic implications. *Epigenomics* 2016, 8, 1151–67. doi:10.2217/epi.16.10.
26. Imyanitov EN, Iyevleva AG, Levchenko EV. Molecular testing and targeted therapy for non-small cell lung cancer: current status and perspectives. *Crit Rev Oncol Hematol* 2021, 157, 103194. doi:10.1016/j.critrevonc.2020.103194.
27. McCarthy F, Roshani R, Steele J, Hagemann T. Current clinical immunotherapy targets in advanced nonsmall cell lung cancer (NSCLC). *J Leukoc Biol* 2013, 94, 1201–6. doi:10.1189/jlb.0313121.
28. Kimura K, Endo Y, Yonemura Y, Heizmann CW, Schafer BW, Watanabe Y, et al. Clinical significance of S100A4 and E-cadherin-related adhesion molecules in non-small cell lung cancer. *Int J Oncol* 2000, 16, 1125–31. doi:10.3892/ijo.16.6.1125.
29. Qi RX, Xu XY. [Inverse correlation of S100A4 and E-cad protein expression and their clinical significance in non-small cell lung cancer]. *Zhonghua Zhong Liu Za Zhi* 2007, 29, 681–4.
30. Treese C, Hartl K, Pötzsch M, Dahlmann M, von Winterfeld M, Berg E, et al. S100A4 is a strong negative prognostic marker and potential therapeutic target in adenocarcinoma of the stomach and esophagus. *Cells* 2022, 11, 1056. doi:10.3390/cells11061056.
31. Ren W, Chi YB, Sun JL. Effect of shRNA-mediated regulation of S100A4 gene expression on proliferation and apoptosis of KLE endometrial cancer cells. *Clin Transl Oncol* 2021, 23, 148–54. doi:10.1007/s12094-020-02406-7.
32. Yang D, Du G, Xu A, Xi X, Li D. Expression of miR-149-3p inhibits proliferation, migration, and invasion of bladder cancer by targeting S100A4. *Am J Cancer Res* 2017, 7, 2209–19.
33. Lyu T, Wang Y, Li D, Yang H, Qin B, Zhang W, et al. Exosomes from BM-MSCs promote acute myeloid leukemia cell proliferation, invasion and chemoresistance via upregulation of S100A4. *Exp Hematol Oncol* 2021, 10, 24. doi:10.1186/s40164-021-00220-7.
34. Tang XH, Guo T, Gao XY, Wu XL, Xing XF, Ji JF, et al. Exosome-derived noncoding RNAs in gastric cancer: functions and clinical applications. *Mol Cancer* 2021, 20, 99. doi:10.1186/s12943-021-01396-6.

35. Rizwan MN, Ma Y, Nenkov M, Jin L, Schröder DC, Westermann M, et al. Tumor-derived exosomes: key players in non-small cell lung cancer metastasis and their implication for targeted therapy. *Mol Carcinog* 2022, 61, 269–80. doi:10.1002/mc.23378.
36. Nikfarjam S, Rezaie J, Kashanchi F, Jafari R. Dexosomes as a cell-free vaccine for cancer immunotherapy. *J Exp Clin Cancer Res* 2020, 39, 258. doi:10.1186/s13046-020-01781-x.
37. Mathew M, Zade M, Mezghani N, Patel R, Wang Y, Momen-Heravi F. Extracellular vesicles as biomarkers in cancer immunotherapy. *Cancers (Basel)* 2020, 12, 2825. doi:10.3390/cancers12102825.
38. Zhou W, Xu M, Wang Z, Yang M. Engineered exosomes loaded with miR-449a selectively inhibit the growth of homologous non-small cell lung cancer. *Cancer Cell Int* 2021, 21, 485. doi:10.1186/s12935-021-02157-7.
39. Chen S, Crabill GA, Pritchard TS, McMiller TL, Wei P, Pardoll DM, et al. Mechanisms regulating PD-L1 expression on tumor and immune cells. *J ImmunoTher Cancer* 2019, 7, 305. doi:10.1186/s40425-019-0770-2.
40. Liu W, Liu R, Yuan R, Wang X. MicroRNA-4458 regulates PD-L1 expression to enhance anti-tumor immunity in NSCLC via targeting STAT3. *Mol Biotechnol* 2021, 63, 1268–79. doi:10.1007/s12033-021-00379-8.
41. Abdelhamed S, Ogura K, Yokoyama S, Saiki I, Hayakawa Y. AKT-STAT3 pathway as a downstream target of EGFR signaling to regulate PD-L1 expression on NSCLC cells. *J Cancer* 2016, 7, 1579–86. doi:10.7150/jca.14713.
42. Zheng Q, Dong H, Mo J, Zhang Y, Huang J, Ouyang S, et al. A novel STAT3 inhibitor W2014-S regresses human non-small cell lung cancer xenografts and sensitizes EGFR-TKI acquired resistance. *Theranostics* 2021, 11, 824–40. doi:10.7150/thno.49600.
43. Li Q, Dai C, Xue R, Wang P, Chen L, Han Y, et al. S100A4 protects myeloid-derived suppressor cells from intrinsic apoptosis via TLR4-ERK1/2 signaling. *Front Immunol* 2018, 9, 388. doi:10.3389/fimmu.2018.00388.
44. Rui K, Hong Y, Zhu Q, Shi X, Xiao F, Fu H, et al. Olfactory ecto-mesenchymal stem cell-derived exosomes ameliorate murine Sjögren's syndrome by modulating the function of myeloid-derived suppressor cells. *Cell Mol Immunol* 2021, 18, 440–51. doi:10.1038/s41423-020-00587-3.
45. Wang K, Wang J, Wei F, Zhao N, Yang F, Ren X. Expression of TLR4 in non-small cell lung cancer is associated with PD-L1 and poor prognosis in patients receiving pulmonectomy. *Front Immunol* 2017, 8, 456. doi:10.3389/fimmu.2017.00456.
46. Kang X, Li P, Zhang C, Zhao Y, Hu H, Wen G. The TLR4/ERK/PD-L1 axis may contribute to NSCLC initiation. *Int J Oncol* 2020, 57, 456–65. doi:10.3892/ijo.2020.5068.
47. Wang K, Wang J, Liu T, Yu W, Dong N, Zhang C, et al. Morphine-3-glucuronide upregulates PD-L1 expression via TLR4 and promotes the immune escape of non-small cell lung cancer. *Cancer Biol Med* 2021, 18, 155–71. doi:10.20892/j.issn.2095-3941.2020.0442.
48. Wen ZF, Liu H, Gao R, Zhou M, Ma J, Zhang Y, et al. Tumor cell-released autophagosomes (TRAPs) promote immunosuppression through induction of M2-like macrophages with increased expression of PD-L1. *J ImmunoTher Cancer* 2018, 6, 151. doi:10.1186/s40425-018-0452-5.
49. Pucci M, Raimondo S, Urzì O, Moschetti M, Di Bella MA, Conigliaro A, et al. Tumor-derived small extracellular vesicles induce pro-inflammatory cytokine expression and PD-L1 regulation in M0 macrophages via IL-6/STAT3 and TLR4 signaling pathways. *Int J Mol Sci* 2021, 22, 12118. doi:10.3390/ijms222212118.
50. Katte RH, Chou RH, Yu C. Pentamidine inhibit S100A4 - p53 interaction and decreases cell proliferation activity. *Arch Biochem Biophys* 2020, 691, 108442. doi:10.1016/j.abb.2020.108442.
51. Ishikawa M, Osaki M, Yamagishi M, Onuma K, Ito H, Okada F, et al. Correlation of two distinct metastasis-associated proteins, MTA1 and S100A4, in angiogenesis for promoting tumor growth. *Oncogene* 2019, 38, 4715–28. doi:10.1038/s41388-019-0748-z.
52. Zhu Y, Zhou Y, Zhou X, Guo Y, Huang D, Zhang J, et al. S100A4 suppresses cancer stem cell proliferation via interaction with the IKK/NF-κB signaling pathway. *BMC Cancer* 2018, 18, 763. doi:10.1186/s12885-018-4563-7.
53. Hua T, Wang X, Chi S, Liu Y, Feng D, Zhao Y, et al. Estrogen-related receptor γ promotes the migration and metastasis of endometrial cancer cells by targeting S100A4. *Oncol Rep* 2018, 40, 823–32. doi:10.3892/or.2018.6471.
54. Zhang XW, Li L, Hu WQ, Hu MN, Tao Y, Hu H, et al. Neurokinin-1 receptor promotes non-small cell lung cancer progression through transactivation of EGFR. *Cell Death Dis* 2022, 13, 41. doi:10.1038/s41419-021-04485-y.
55. Zhang Y, Ma P, Duan Z, Liu Y, Mi Y, Fan D. Ginsenoside Rh4 suppressed metastasis of lung adenocarcinoma via inhibiting JAK2/STAT3 signaling. *Int J Mol Sci* 2022, 23, 2018. doi:10.3390/ijms23042018.
56. Su H, Fan G, Huang J, Qiu X. LncRNA HOXC-AS3 promotes non-small-cell lung cancer growth and metastasis through upregulation of YBX1. *Cell Death Dis* 2022, 13, 307. doi:10.1038/s41419-022-04723-x.
57. Ullah A, Leong SW, Wang J, Wu Q, Ghauri MA, Sarwar A, et al. Cephalomannine inhibits hypoxia-induced cellular function via the suppression of APEX1/HIF-1α interaction in lung cancer. *Cell Death Dis* 2021, 12, 490. doi:10.1038/s41419-021-03771-z.